18th International Conference on Structural Mechanics in Reactor Technology (SMiRT 18)
Beijing, China, August 7-12, 2005
SMiRT18-K10-3

RESEARCH ON 3-D BASE ISOLATION SYSTEM APPLIED TO NEW POWER REACTOR
3-D SEISMIC ISOLATION DEVICE WITH ROLLING SEAL TYPE AIR SPRING: PART 2

Junji Suhara
Shimizu Corporation,No.2-3, Shibaura 1-chome, Minato-ku, Tokyo 105-8007, Japan
Phone:+81-3-5441-0859,Fax:+81-3-5441-0370
E-mail: junji-suhara@shimz.co.jp

Ryoichiro Matsumoto
Shimizu Corporation, Japan
Phone:+81-3-5441-0859,Fax:+81-3-5441-0370
E-mail: matsumotor@shimz.co.jp

Shinsuke Oguri
Shimizu Corporation, Japan
Phone:+81-3-5441-0859,Fax:+81-3-5441-0370
E-mail: guri@shimz.co.jp

Yasuo Okada
Shimizu Corporation, Japan
Phone:+81-3-5441-0859,Fax:+81-3-5441-0370
E-mail: okapi@shimz.co.jp

Kazuhiko Inoue
The Japan Atomic Power Company, Japan
Phone:+81-29-267-4141,Fax:+81-29-267-7173
E-mail: inoue.kazuhiko@jnc.go.jp

Kenji Takahashi
The Japan Atomic Power Company, Japan
Phone:+81-29-267-4141,Fax:+81-29-266-3675
E-mail: takahashi.kenji@jnc.go.jp

ABSTRACT

A three dimensional seismic base isolation device was developed for heavy structures and buildings such as nuclear power reactor buildings. The device realizes 3-D isolation by combining a LRB (laminated rubber bearing) for horizontal isolation with an air spring for vertical isolation in series. In this study, scale models of the 3-D base isolation device were made and were tested to examine the dynamic properties and ultimate strengths of the device.

The performance of the device under earthquake excitation was examined through shaking table tests of 1/7 scale models. As the results, it was confirmed that the device worked smoothly under the horizontal and vertical excitations, and that the theoretical formulae of the orifice damping could explain the test results.

The high-pressure air springs of trial production were forced to burst to find out which factor influenced ultimate strength. It was confirmed from results of the burst test that the strength of the air spring depended upon the diameter of rolling part of the bellows and the number of layers of the reinforcing fibers.

Judging from the results of the shaking table test and the burst test, the developed 3-D base isolation device was applicable to a nuclear power plant building.

Keywords: Shaking table test, Seismic base isolation, LRB, Air spring, 3-D

INTRODUCTION

A 3-D seismic isolation device was developed to use as a base isolation system for a heavy building like a nuclear power reactor building. The 3-D seismic isolation device consists of a laminated rubber bearing with a lead plug (LRB) and a rolling seal type air spring placed in series.

Both LRBs and air springs are reliable, as they are individually used for ordinary buildings and industrial structures widely. However, when these two components are combined, the following points should be checked.

1) Performance of the device, when vertical force and horizontal force acted simultaneously
2) Capability of supporting excessive weight
3) Damping performance to reduce vibration

The performance and the applicability of the 3-D base isolation device itself were already studied in feasibility tests (Suhara,2002, Suhara,2003, Hagiwara,2004). In this paper, results of the shaking table test, in which the base isolation system was demonstrated to function smoothly, and the burst test of high-pressure air springs are presented.

THREE-DIMENSIONAL (3-D) SEISMIC BASE ISOLATION DEVICE

The concept of the 3-D seismic isolation device is outlined in Fig.1. Dynamic properties and specifications of the device are summarized in Table 1. These dynamic properties are determined from the results of earthquake response analysis of an actual nuclear power plant (Kato,2002). The device realizes 3-D isolation by combining LRB for horizontal isolation with the air spring for vertical isolation.

The specifications of the LRB were determined from the results of the previous research (Kato, 1995). The air spring is set in the lower basemat. A rolling seal type air spring was adopted, because the stroke of the air spring should be long enough so that the device can be in operation even after experiencing large vertical deformation. The contact region shall be designed so that the horizontal force can be transmitted with small friction. Regular pressure of the air spring is 1.6MPa, which is relatively high compared with the pressure of an ordinary air spring (about 0.3-0.9 MPa). Therefore, the long-term reliability of the air spring using high pressure is important.

Horizontal damping performance is provided by the lead plug of the LRB. Vertical damping performance is provided by the orifice damping and viscous damping of the oil damper, which is set at the perimeter zone of the basemat.

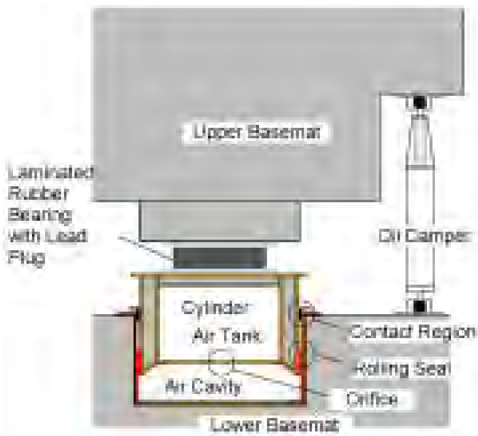

Fig. 1 Concept of 3-D Isolation Device

Table 1 Outline of 3-D Seismic Isolation Device

Dynamic Properties	Horizontal Initial Period	1.0 s
	Horizontal Isolation Period	2.8 s
	Horizontal Yield Coefficient	0.1
	Vertical Isolation Period	2.0 s
	Vertical Damping Factor	0.2
Specifications	Supporting Load	9800kN
	Diameter of Rubber Bearing	1.6 m
	Total rubber thickness	0.225m
	Diameter of Air Cavity	3.0m
	Pressure of Air Cavity	1.6MPa

SHAKING TABLE TEST

(1) SIMILARITY LAW

The similarity law used in this study is shown in Table 2. Both acceleration and density of the model are equal to those of the prototype in this similarity law. The scale ratio of the model to an actual prototype device is 1:7.

Table 2 Similarity Law

Parameter	Similitude	$\lambda=7$
Length	$1/\lambda$	1/7
Velocity	$1/\lambda^{1/2}$	1/2.7
Acceleration	1	1
Time	$1/\lambda^{1/2}$	1/2.7
Mass	$1/\lambda^{3}$	1/343
Stress	$1/\lambda$	1/7
Density	1	1

(2) DESIGN OF TEST MODEL

a. LRB for the Test Model

The sectional view and specification of the LRB with a lead plug used in the model are shown in Fig.2 and Table 3. Since the similarity law summarized in Table 2, in which the density of the model is equal to that of the prototype, is adopted, the shape of the LRB for the model is more slender than the LRB for prototype.

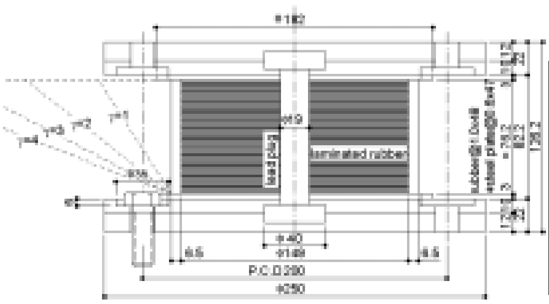

Fig.2 LRB used in Test Model

Table 3 Dimension of Laminated Rubber Bearing

Parameter	Prototype	Model
Support load (kN)	9800	28.9
Horizontal isolation period (s)	2.8	1.07
Diameter of LRB (m)	1.72	1.49
Total rubber thickness (m)	0.23	0.048
Diameter of lead plug (m)	0.35	0.019
Axial stress (MPa)	4.4	0.83

b. Test Model of Air spring

The sectional view and specification of the air spring model are shown in Fig.3 and Table 4.

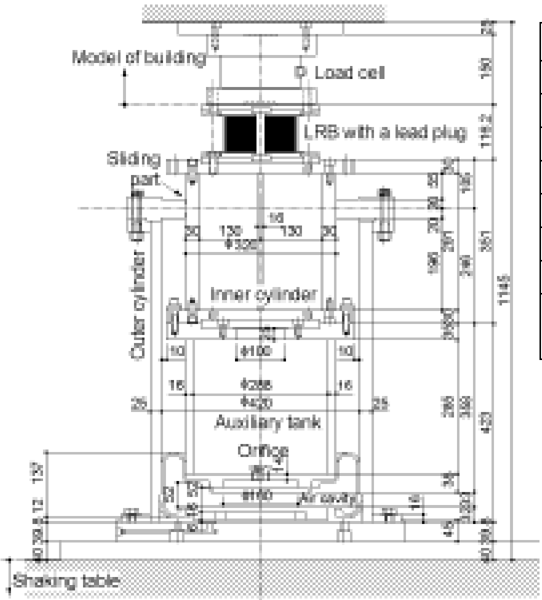

Fig.3 Test Model of Air Spring

Table 4 Dimension of Air Spring

Parameter	Prototype	Model
Support load (kN)	9800	28.6
Vertical isolation period (s)	2.0	0.76
Pressure of air cavity (MPa)	1.6	0.26
Effective diameter of air cavity (m)	2.82	0.37
Maximum stroke (mm)	600	50
Volume of air spring (m3)	9.4	0.03
Volumetric ratio of auxiliary tank to air cavity	1:1	1:1.65

c. Test Model of Oil Damper

The shape and specification of an oil damper are shown in Fig.4 and Table 5.

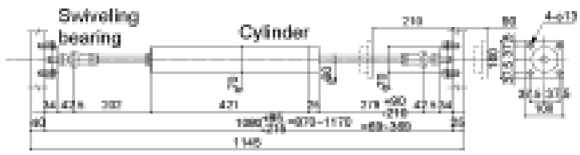

Fig.4 Test Model of Oil Damper

Table 5 Dimension of Oil Damper

Parameter	Prototype	Model
Damping factor (%)	20*	10*
Vertical natural period (s)	2.0	0.76
Damping coefficient (kN·s/m)	1260	4.9
Design stroke (mm)	900	129
Design velocity (m/s)	2.83	1.07
Design damping force (kN)	3500	5.2

* : Two models correspond to one prototype damper

d. Test Model of Building and Pantagraph type rocking suppression device

The weight which represents the building consists of steel plates and steel frame to support plates. Size of the weight is 2.35m in horizontal direction. Mass of the weight is 11.66t. Height of the center of the mass is 1/3.5 of horizontal length (=2.35m) measured from the center level of the LRBs. A pantagraph type rocking suppression device which is made of steel pipes and bearings is attached to the steel frame. Sectional view of the building model and a pantograph types rocking suppression device are shown in Fig.5.

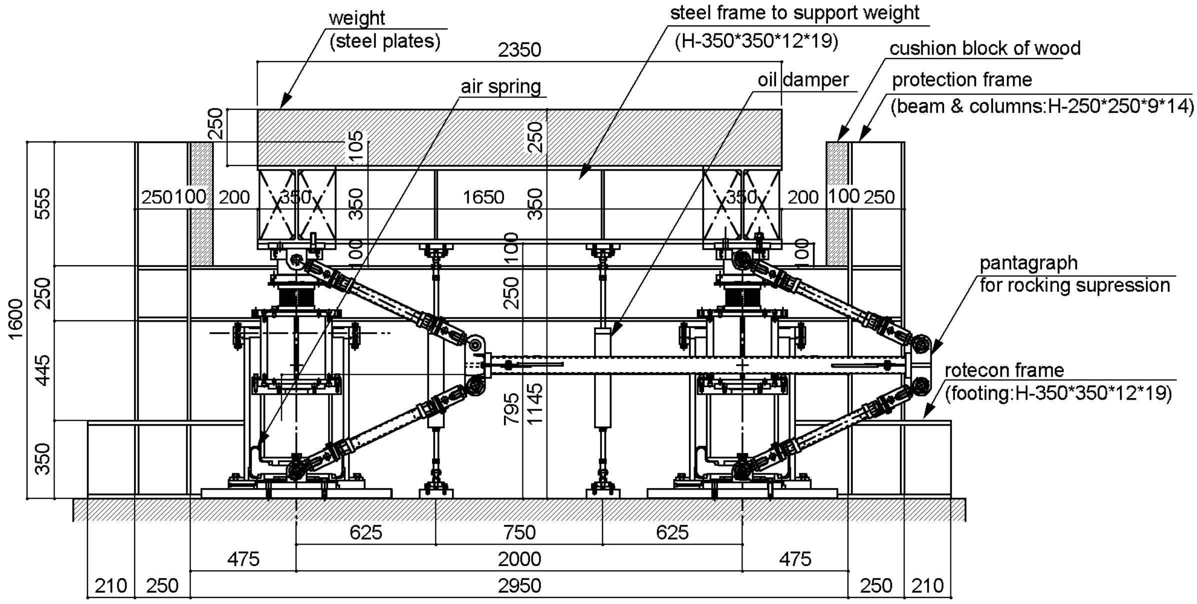

Fig.5 Setup of Test Model

e. Photographs of Shaking Table Test

The model used for the shaking table test consists of four air springs, four oil dampers, and a rigid body building model which weighs 114kN. The photographs of the test model are shown in Photo.1.

Photo.1 View of Shaking Table Test

(3) SINUSOIDAL EXCITATION TEST

Transfer functions and hysteresis loops of vertical response to sinusoidal excitation are shown in Fig.6 and 7. Figure 6 shows the case where the acceleration amplitude of the input sinusoidal wave is 20Gal, and Figure 7 is the case of 100Gal input.

Four lines for four air springs are plotted in each graph of transfer functions. In case of hysteresis loops, averaged data of four air springs are plotted. Amplitude of the transfer functions become largest at frequency of 1.4Hz. Phase angle of the transfer functions become -90deg. at the frequency a little bit higher than 1.4Hz. Curves of the hysteresis loops look smooth even in the case of 20Gal input. It is clear that orifice damping becomes large, as amplitude becomes large.

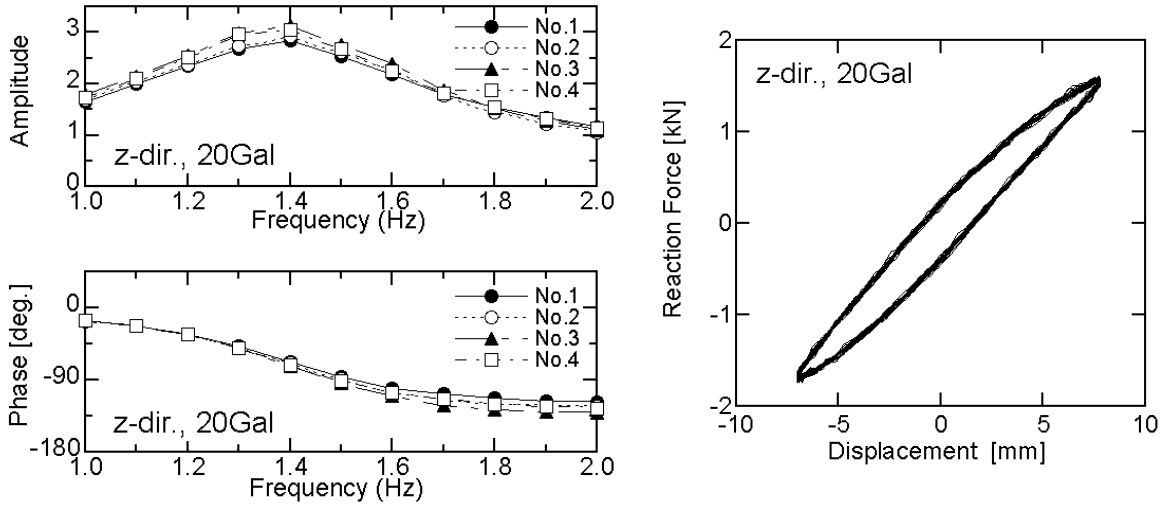

a. Transfer Function   b. Vertical Hysteresis Loop

Fig.6 Response of Sine Wave Excitation (maximum input acceleration is 20Gal)

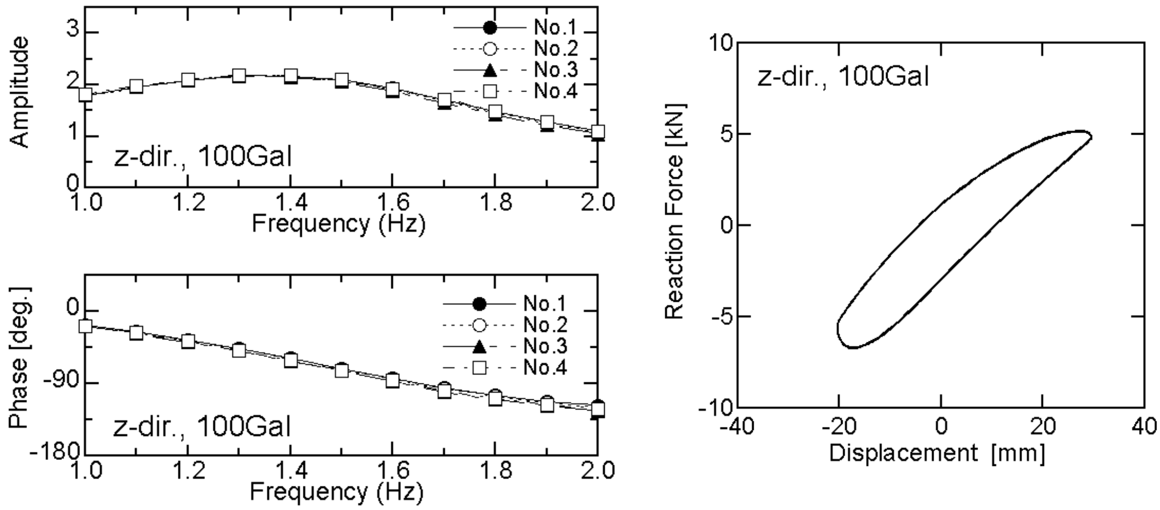

a. Transfer Function   b. Vertical Hysteresis Loop

Fig.7 Response of Sine Wave Excitation (maximum input acceleration is 100Gal)

(4) INPUT EARTHQUAKE WAVES

An artificial earthquake wave S_2, velocity response spectra (h=5%) of which reaches 2m/s in horizontal direction and 1.2m/s in vertical direction, was made in the preceding study (Kato, 1995). In this study, the earthquake wave S_2 is adopted as the greatest seismic excitation. Because of restrictions of the shaking table capacities, band-pass filtered S_2 wave was used if horizontal wave and vertical wave were input simultaneously.

Pass band of the digital filter is set to be 0.794Hz-3.44Hz, so that frequency components dominant for seismic isolation devices were not reduced.

Time history waves and response spectra of the original S_2 waves, scaled S_2 waves, and band-pass filtered S_2 waves are shown in Fig.8 and Fig.9. Upper scale of x-axis in Fig.9 shows frequency in prototype.

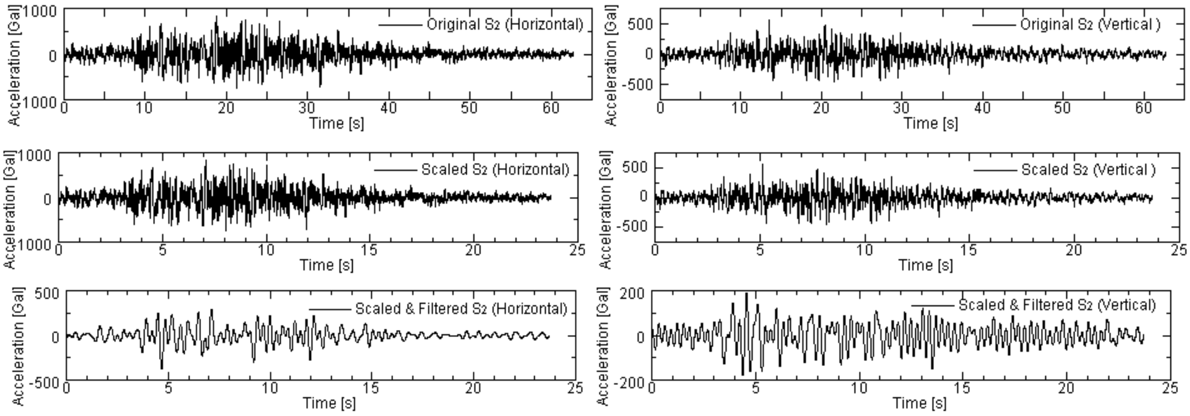

Fig.8 Acceleration Time History of Input Earthquake Waves

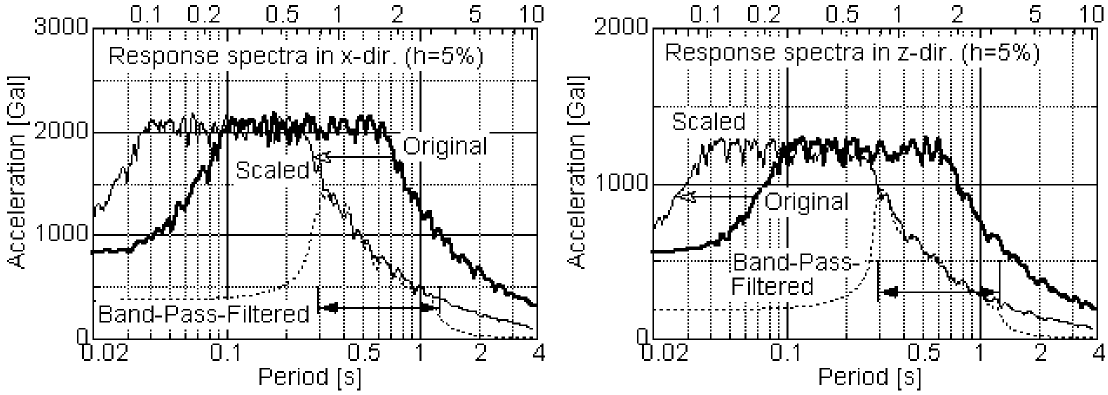

b. Acceleration Response Spectra

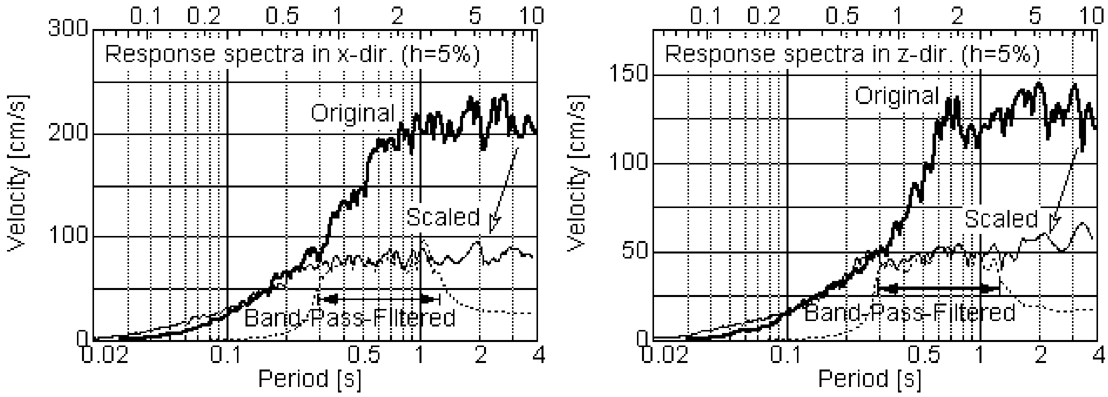

c. Velocity Response Spectra

Fig.9 Response Spectra of Input Earthquake Waves

(5) EARTHQUAKE WAVE EXCITATION TEST

Hysteresis loops of vertical response to earthquake excitation are shown in Fig.10 and Fig.11. The response to vertical input and the response to vertical and horizontal input are compared in these figures. Figure 10 shows the response to S_2(filtered) input and Fig.11 shows that of 1.5*S_2(filtered) input. Acceleration response spectra of the same cases are plotted in Fig.12. Upper scale of x-axis in these graphs shows frequency in prototype. It is obvious from these figures that horizontal response has little influence on vertical response in this test. Also plotted in Fig.13 are hysteresis loops and time history wave of response to non-filtered original input wave.

Response spectra are shown in Fig.12 and Fig.13. Though effect of base isolation is not so obvious in case of band-pass filtered S_2 wave as high frequency components of input wave were small, most of these high frequency components are cut by the isolation device, as is shown in Fig.13.

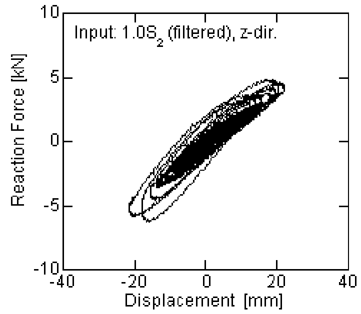

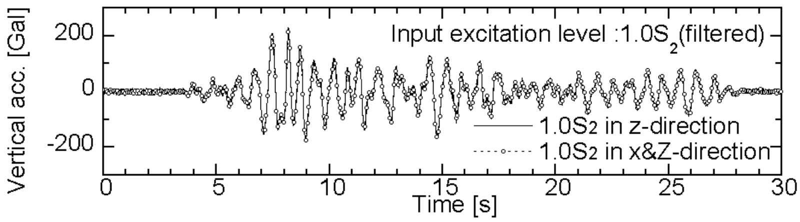

b. Time history of response acceleration

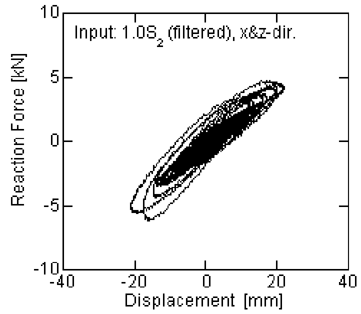

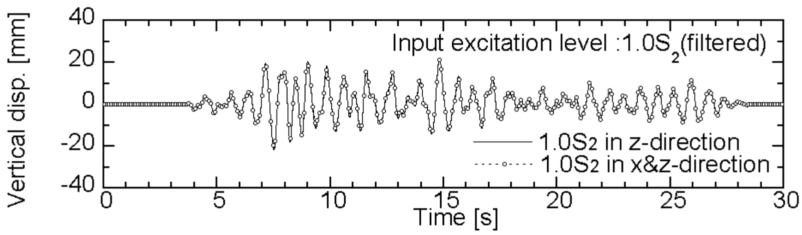

c. Time history of response displacement

a. Hysteresis loop

Fig.10 Vertical Response to Earthquake Excitation (Input: S2, Filtered Wave)

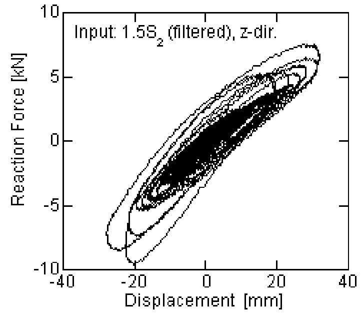

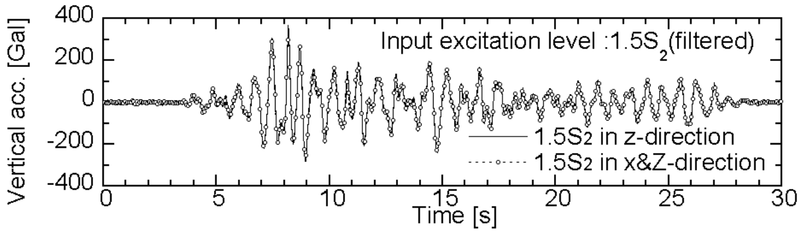

b. Time history of response acceleration

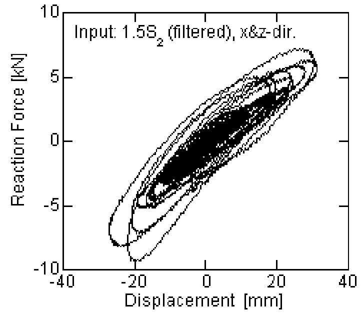

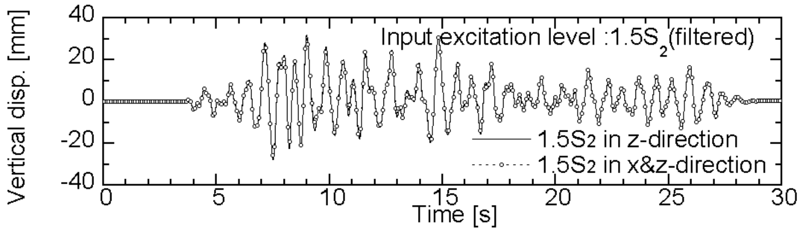

c. Time history of response displacement

a. Hysteresis loop

Fig.11 Vertical Response to Earthquake Excitation (Input:1.5S2, Filtered Wave)

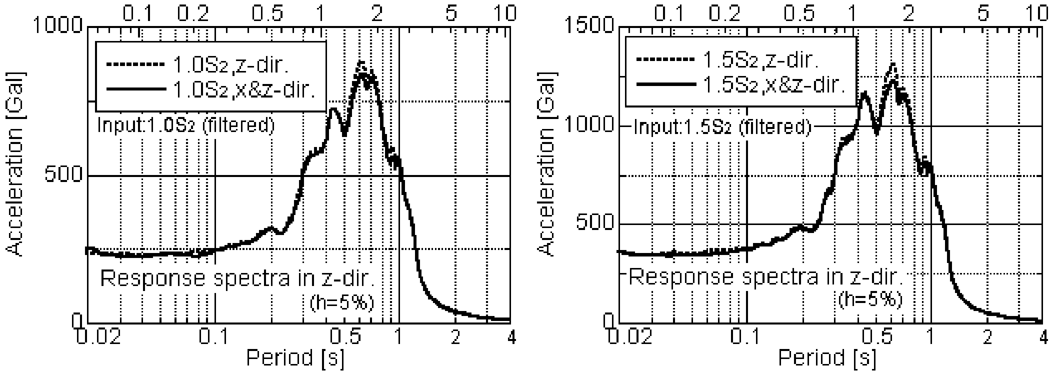

Fig.12 Influence of Horizontal Input on Vertical Response Spectra

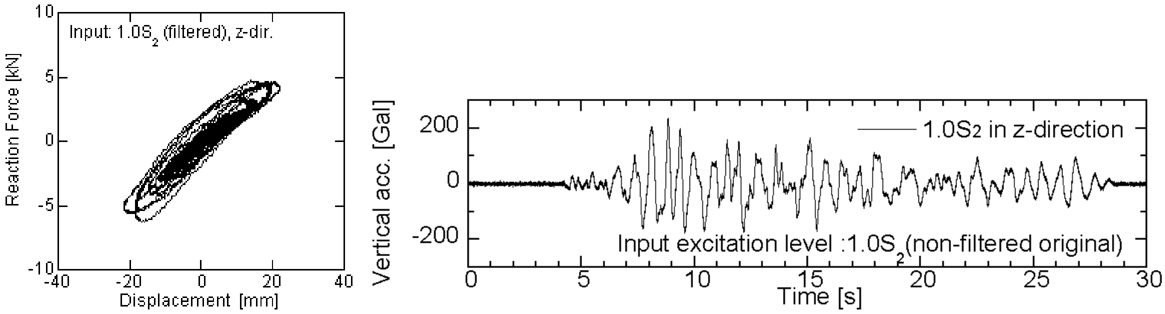

a. Hysteresis loop b. Time history of response acceleration

Fig.13 Vertical Response to Non-filtered Original Earthquake Excitation

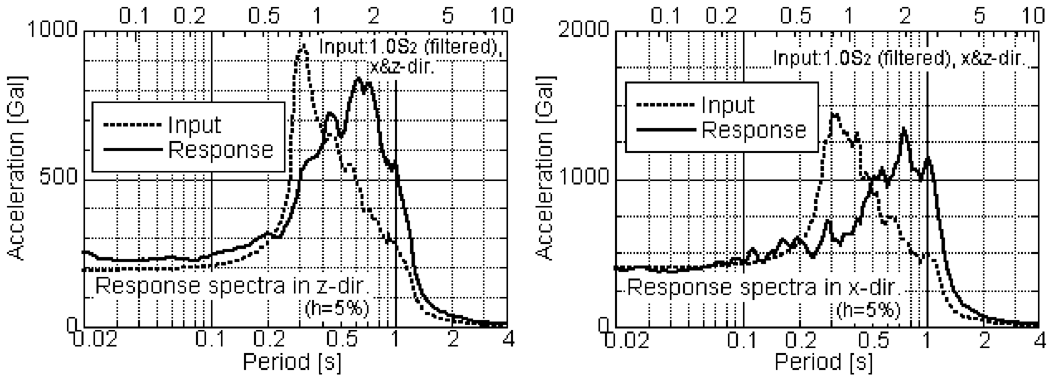

a. Vertical b. Horizontal

Fig.14 Response Spectra (Input:1.0S2, filtered wave)

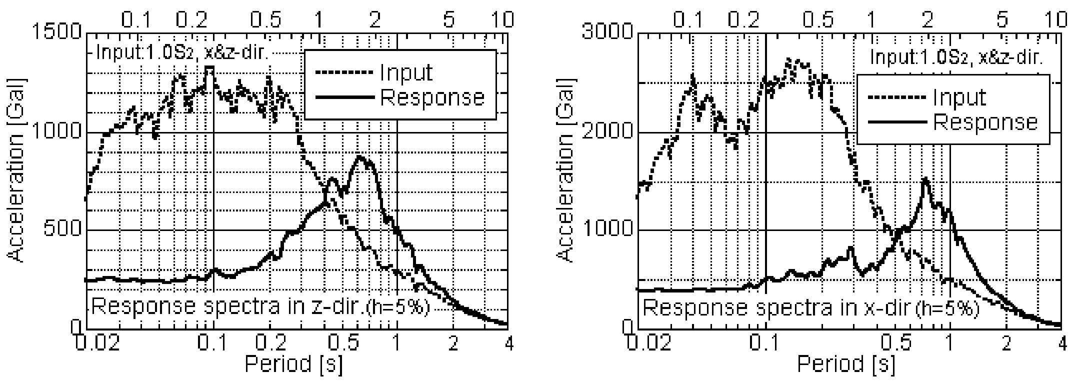

a. Vertical b. Horizontal

Fig.15 Response Spectra (Input:1.0S2, non-filtered original wave)

(6) SIMULATION ANALYSIS OF EARTHQUAKE EXCITATION TEST

The response of the test model was calculated by the analysis model shown in Fig.16. Results of calculation are shown in Fig.17 and Fig.18. Though the air spring shows weak non-linearity and the stiffness for downward displacement increment is higher than that for upward displacement increment, the analysis model used here is so simple to ignore this fact. Thus calculated results slightly differ from experimental results, it is possible to get reasonable estimation of the response of the base isolated building by this quite simple analysis.

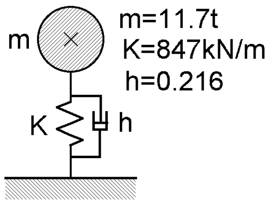

Fig.16 Analysis Model

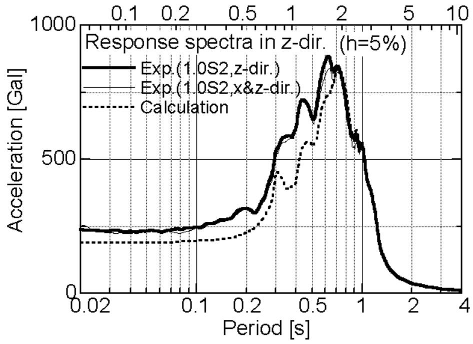

Fig.17 Response Spectra

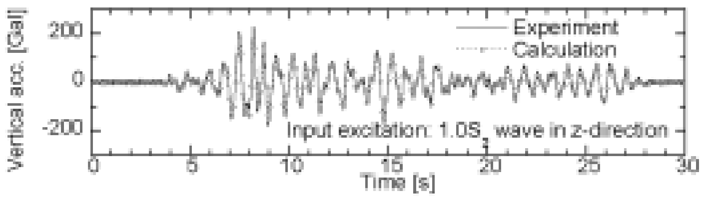

a. Vertical Acceleration

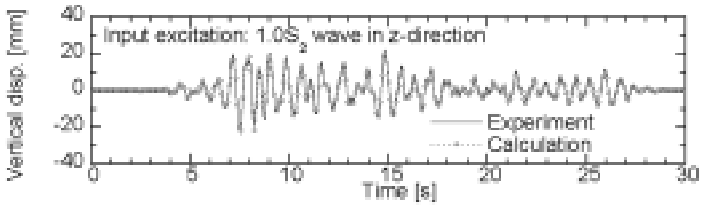

b. Vertical Displacement

Fig.18 Time History of Calculated Response Compared to Experiment

BURST TEST OF AIR SPRINGS

It is possible to cut down the size of the device, if high-pressure air springs are available. Adoption of the high-pressure air springs leads to easiness of fabrication and maintenance of the device and cost down. It is also possible to expect greater margin regarding ultimate strength.

To examine the ultimate pressure and failure mode of the rubber bellows of the air spring, burst test was done. Setup of the test is shown in Fig.19 and Photo.2. After pouring water into the air spring, vertical load was applied to bring the air spring to burst. The test results are summarized in Fig.20 and Table 6. The shape of the burst air spring is shown in Photo.3.

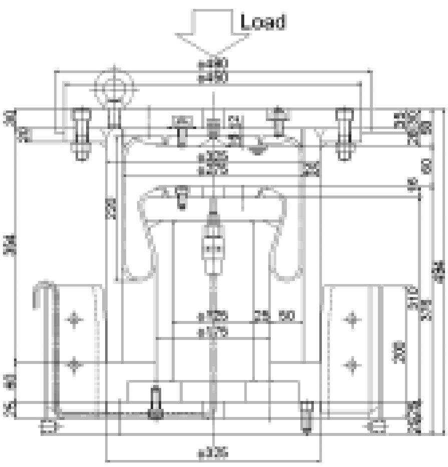

Fig.19 Setup of Burst Test

Photo.2 Test Machine

Photo.3 Air Spring Bellows After Burst

The strength of air spring becomes high, if the diameter of rolling part of the air spring is small, the initial gap is small, or rubber bellows of the air spring is reinforced enough.

From these test results, it is proved that the air spring, the maximum pressure of which exceeds 20MPa, can be made.

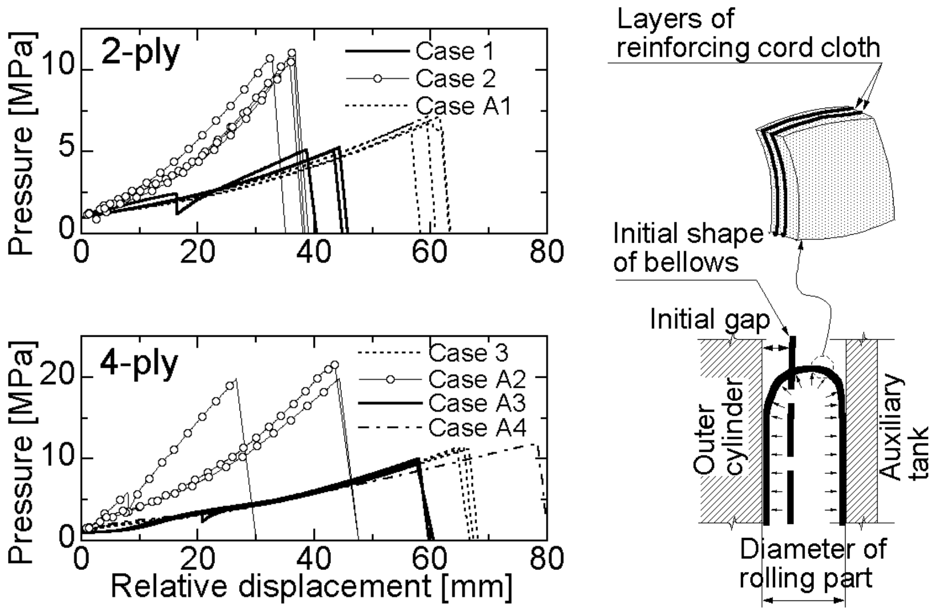

Fig.20 Displacement-Pressure Curves

Table 6 Burst Pressure of Air Springs

#	Diameter of rolling part (mm)	Ply of reinforcing cord cloth	Initial gap (mm)	Bead wire arrangement	Maximum pressure (MPa)	Failure mode
1	50	2	29	4x4 loops	5.15 5.28 5.11	bellows
2	30	2	16	4x4 loops	10.89 11.26 10.41	bellows
3	50	4	16	4x5 loops	11.38 11.19 11.37	bead
A1	50	2	16	4x4 loops	6.71	bead
					6.77 7.15 7.15	bellows
A2	30	4	16	4x5 loops	19.85 21.75 19.87	bellows
A3	50	4	29	4x5 loops	9.40 10.07 9.76	bellows
A4	50	4	16	4x6 loops	11.90	bead

CONCLUSIONS

Performance of the 3-D seismic isolation devices which used air springs was examined through shaking table tests. The specimen consisted of a weight, four air springs and four oil dampers. Pantographs made of steel pipes and bearings were also attached to the specimen to suppress rocking motion mechanically. Designed values of dynamic properties of the specimen such as natural frequency and damping factor were attained in the test, to prove the performance of the air springs. It was also confirmed that the maximum earthquake response values and floor response spectra in vertical direction were reasonably evaluated by linear response analysis using equivalent damping factor and spring constant.

The high-pressure air springs of trial production were brought to burst to examine strength. The target of the maximum pressure to actualize compact air spring devices was set to be 17.5MPa. Among several cases tested, the specimen of four layers of reinforcement fiber membranes achieved the maximum pressure of 20.5MPa, when the size of the rolling part was set to be 30mm.

As the result of these test, the developed 3-D base isolation system was judged to be applicable to an actual nuclear power plant.

ACKNOWLEDGMENT

This study is a part of project sponsored by the Japanese government (METI) and was conducted by the Japan Atomic Power Company in collaboration with Japan Nuclear Cycle Institute. The authors wish to express their profound appreciation to the project committee members.

REFERENCES

Kato, M., et al., (1995), Design study of the seismic-isolated reactor building of demonstration FBR plant in Japan, 13th SMIRT, pp579-584

Suhara, J., et al., (2002), Development of Three Dimensional Seismic Isolation Device with Laminated Rubber Bearing and Rolling Seal Air Spring, ASME PVP, Seismic Engineering

Kato, A., et al., (2002), A large Scale Ongoing R&D Project on Three-Dimensional Seismic Isolation for FBR in Japan, ASME PVP, Seismic Engineering

Suhara, J., et al., (2003), Research on 3-D Base Isolation System Applied to New Power Reactor 3-D, Seismic Isolation Device with Rolling Seal Type Air Spring : Part 1, 17th SMIRT, K10-2

Tetsuya Hagiwara, et al., (2004), Three-Dimensional Seismic Isolation Device with Rolling Seal Type Air Spring, ASME PVP, Seismic Engineering

